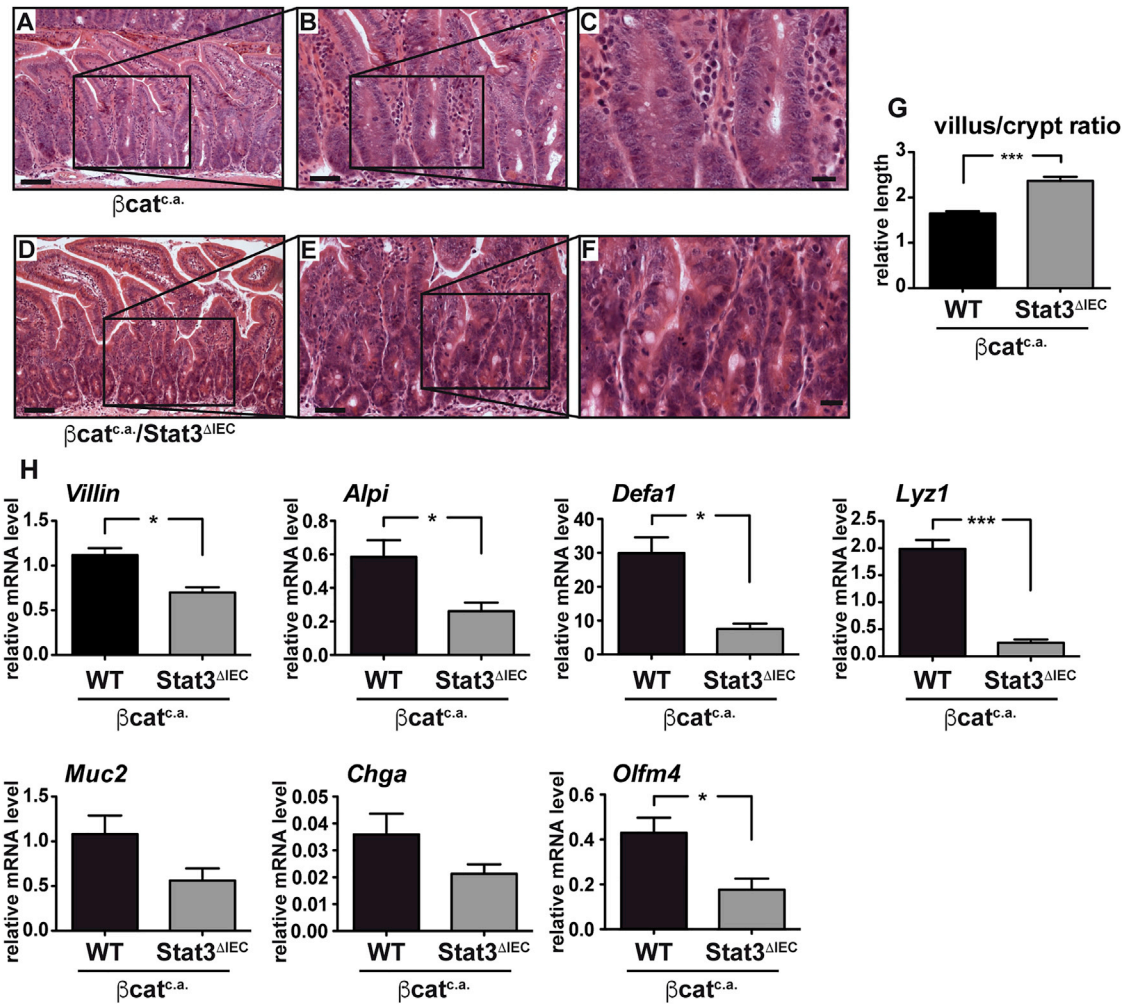

Figure S1. Loss of Stat3 in IEC Does Not Improve IEC Differentiation during Tumorigenesis, Related to Figure 1

(A–F) H&E staining of the small intestine of *β-cat*$^{c.a.}$ (A–C) and *β-cat*$^{c.a}$/Stat3$^{\Delta IEC}$ (D–F) mice 15 days after the start of tamoxifen administration. Scale bar, 100 μm (A and D), 50 μm (B and E), or 20 μm (C and F).

(G) Villus length relative to average crypt length per mouse in the small intestine of *β-cat*$^{c.a.}$ and *β-cat*$^{c.a}$/Stat3$^{\Delta IEC}$ mice 15 days after the start of tamoxifen administration (n = 3 or 5 mice, respectively, ***$p < 0.001$ by Student's t test). Data are mean ± SEM.

(H) Relative mRNA expression of the indicated genes in IEC of *β-cat*$^{c.a.}$ and *β-cat*$^{c.a.}$/*Stat3*$^{\Delta IEC}$ mice 15 days after the start of tamoxifen administration (n = 3 mice per genotype). Data are mean ± SEM.

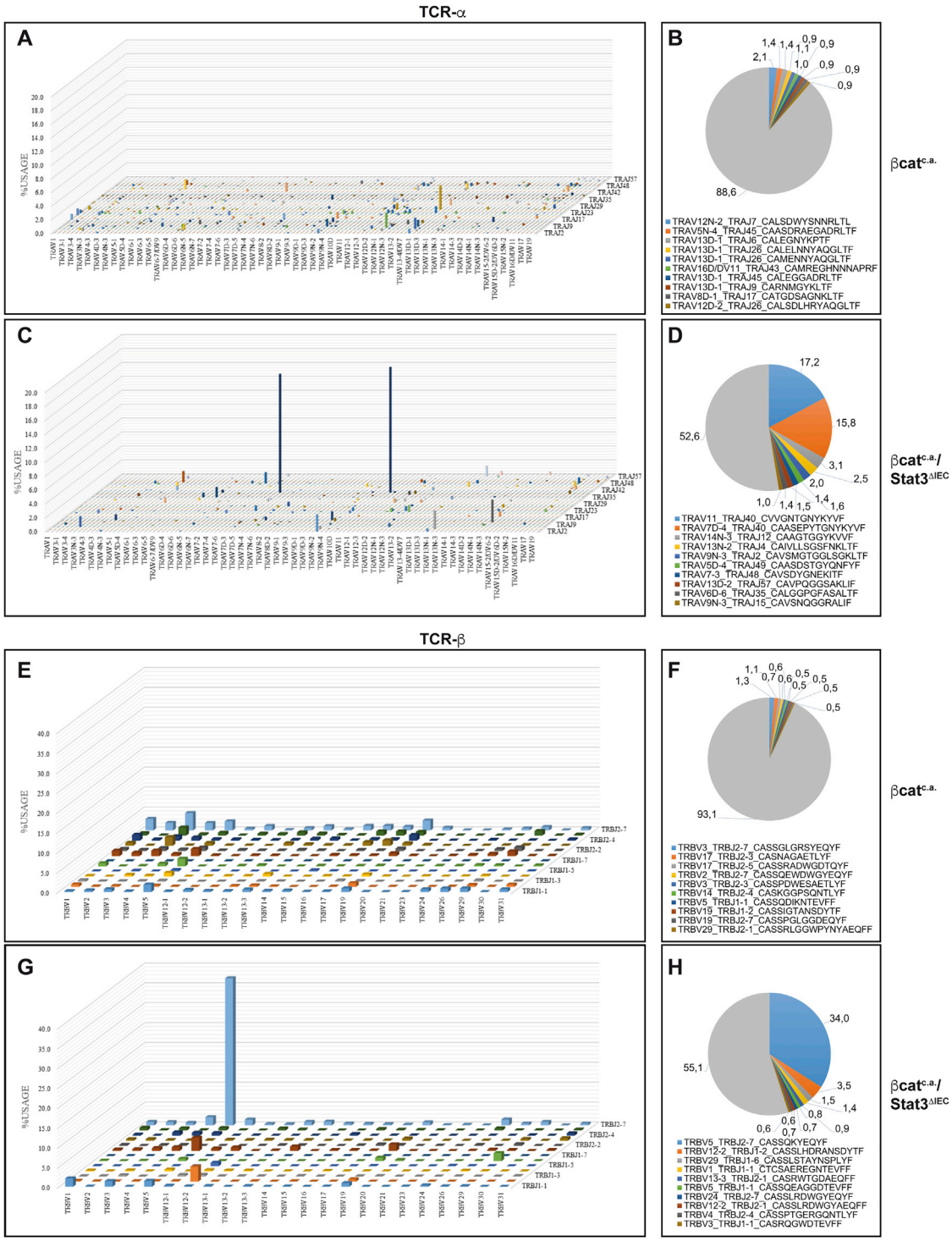

Figure S2. Clonal Expansion of Intestinal CD8$^+$ T Cells in *β-cat*$^{c.a.}$/*Stat3*$^{\Delta IEC}$ Mice, Related to Figure 3

(A–H) CD8$^+$ T cells were sorted from intestines, their RNA was extracted and sequenced for CDR3 regions of TCR-α and TCR-β chain. Panels show the relative abundance of productive unique TCR-α (A–D) and TCR-β (E–H) chain sequences (A, C, E, and G) and the relative contribution of the ten most abundant sequences (B, D, F, and H) from one representative *β-cat*$^{c.a.}$ (A, B, E, and F) and *β-cat*$^{c.a.}$/*Stat3*$^{\Delta IEC}$ mouse (C, D, G, and H) each 15 days after the start of tamoxifen administration (of 3 or 4 mice analyzed, respectively).

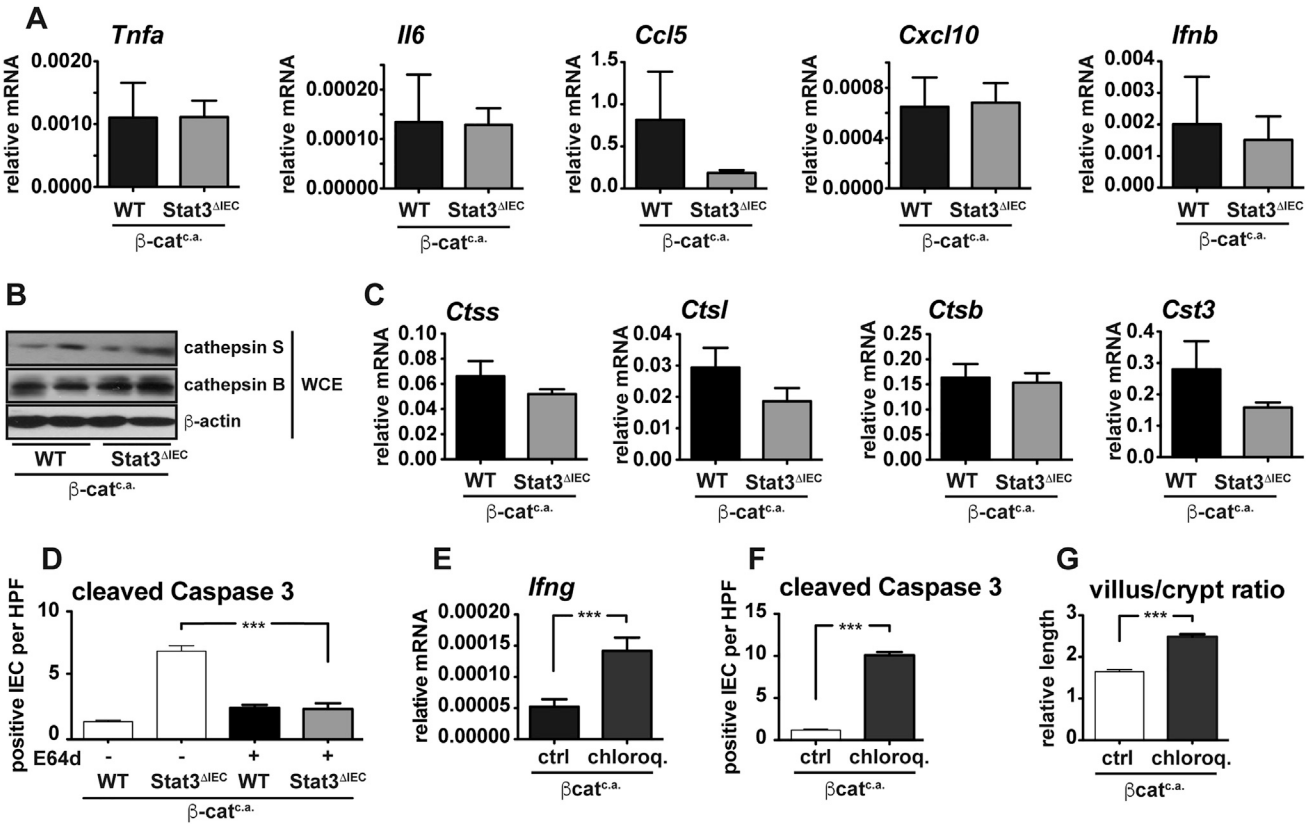

Figure S3. Immune Activation in *β-cat*$^{c.a.}$/*Stat3*$^{\Delta IEC}$ Mice Is Dependent on Cathepsin Activity, Related to Figure 4

(A) Relative mRNA expression of *Tnfa, Il6, Ccl5, Cxcl10 and Ifnb* in small intestinal mucosa of *β-cat*$^{c.a.}$ and *β-cat*$^{c.a.}$/*Stat3*$^{\Delta IEC}$ mice 3 days after the start of tamoxifen administration (n = 5 mice per genotype). Data are mean ± SEM.

(B) Immunoblot analysis of cathepsin S and cathepsin B in whole cell extracts (WCE) of small intestinal IEC of *β-cat*$^{c.a.}$ and *β-cat*$^{c.a.}$/*Stat3*$^{\Delta IEC}$ mice 15 days after the start of tamoxifen administration.

(C) Relative mRNA expression of *Ctss*, *Ctsl*, *Ctsb* and *Cst3* (encoding the cysteine protease inhibitor Cystatin C) in isolated small intestinal IEC of *β-cat*$^{c.a.}$ and *β-cat*$^{c.a.}$/*Stat3*$^{\Delta IEC}$ mice 15 days after the start of tamoxifen administration. (n = 6 mice each, $p > 0.05$ by Student's t test).

(D) Quantification of cleaved caspase-3 positive IEC in the small intestine of E64d-treated or control *β-cat*$^{c.a.}$ or *β-cat*$^{c.a.}$/*Stat3*$^{\Delta IEC}$ mice 15 days after the start of tamoxifen administration (n = 4/group, ≥ 20 400X-high-power fields (HPF) have been counted per animal, ***$p < 0.001$ by Student's t test). Please note that parts of the figure have been reproduced from Figure 2Q for better visibility.

(E) Relative amount of *Ifng*-mRNA in the small intestine of *β-cat*$^{c.a.}$ mice 15 days after the start of tamoxifen administration treated with chloroquine or control (n ≥ 6 per group, ***$p < 0.001$ by Student's t test).

(F) Quantification of cleaved caspase-3 positive IEC in the small intestine of chloroquine-treated or control *β-cat*$^{c.a.}$ mice 15 days after the start of tamoxifen administration (n = 4/group, ≥ 20 400X-high-power fields (HPF) have been counted per animal, ***$p < 0.001$ by Student's t test). Please note that parts of the figure have been reproduced from Figure 2Q for better visibility.

(G) Villus length relative to average crypt length per mouse in the small intestine of chloroquine-treated or control *β-cat*$^{c.a.}$ mice 15 days after the start of tamoxifen administration (n = 3 mice per group, ***$p < 0.001$ by Student's t test). Please note that parts of the figure have been reproduced from Figure S1G for better visibility.

In (C)–(G), data are mean ± SEM.

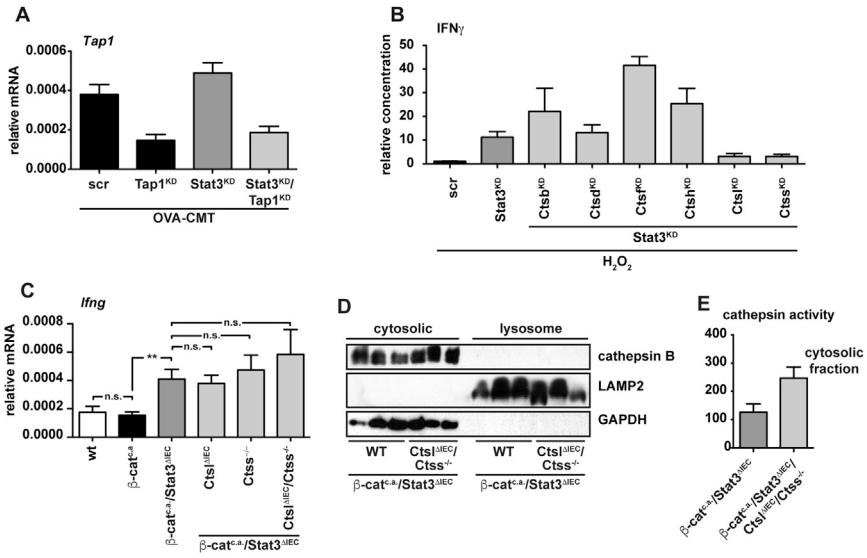

Figure S4. Different Cathepsins Can Compensate for the Loss of Another, Related to Figure 5

(A) OVA-CMT cells have been transfected with the indicated siRNA and analyzed 2 days later for the expression of *Tap1* (data are mean ± SEM, n = 3 each).

(B) IFNγ levels in the supernatant of OT-I splenocytes that had been co-cultured for two days with OVA-CMT cells with RNAi-mediated knockdown of the indicated genes. OVA-CMT cells had been stimulated with H_2O_2 (1 mM) for 2 hr prior to co-culture with OT-I splenocytes (data are mean ± SEM, n ≥ 6 from 3 independent experiments, *p < 0.05, ***p < 0.001).

(C) Relative *Ifng* mRNA expression in small intestinal mucosa of mice with the indicated genotype 15 days after the start of tamoxifen administration. (Data are mean ± SEM, n ≥ 7, **p < 0.01 by Student's t test).

(D) Immunoblot analysis of cathepsin B, LAMP2 and Gapdh in cytosolic and membrane fractions isolated from small intestinal IEC of β-$cat^{c.a.}$/$Stat3^{\Delta IEC}$ and β-$cat^{c.a.}$/$Stat3^{\Delta IEC}$/$Ctsl^{\Delta IEC}$/$Ctss^{-/-}$ mice 3 days after the start of tamoxifen administration.

(E) Protease activity of cytosolic cathepsins as measured using the fluorogenic substrate z-Phe-Leu-AMC (measured in duplicates, data are mean ± SEM from n ≥ 3 mice, *p < 0.05).

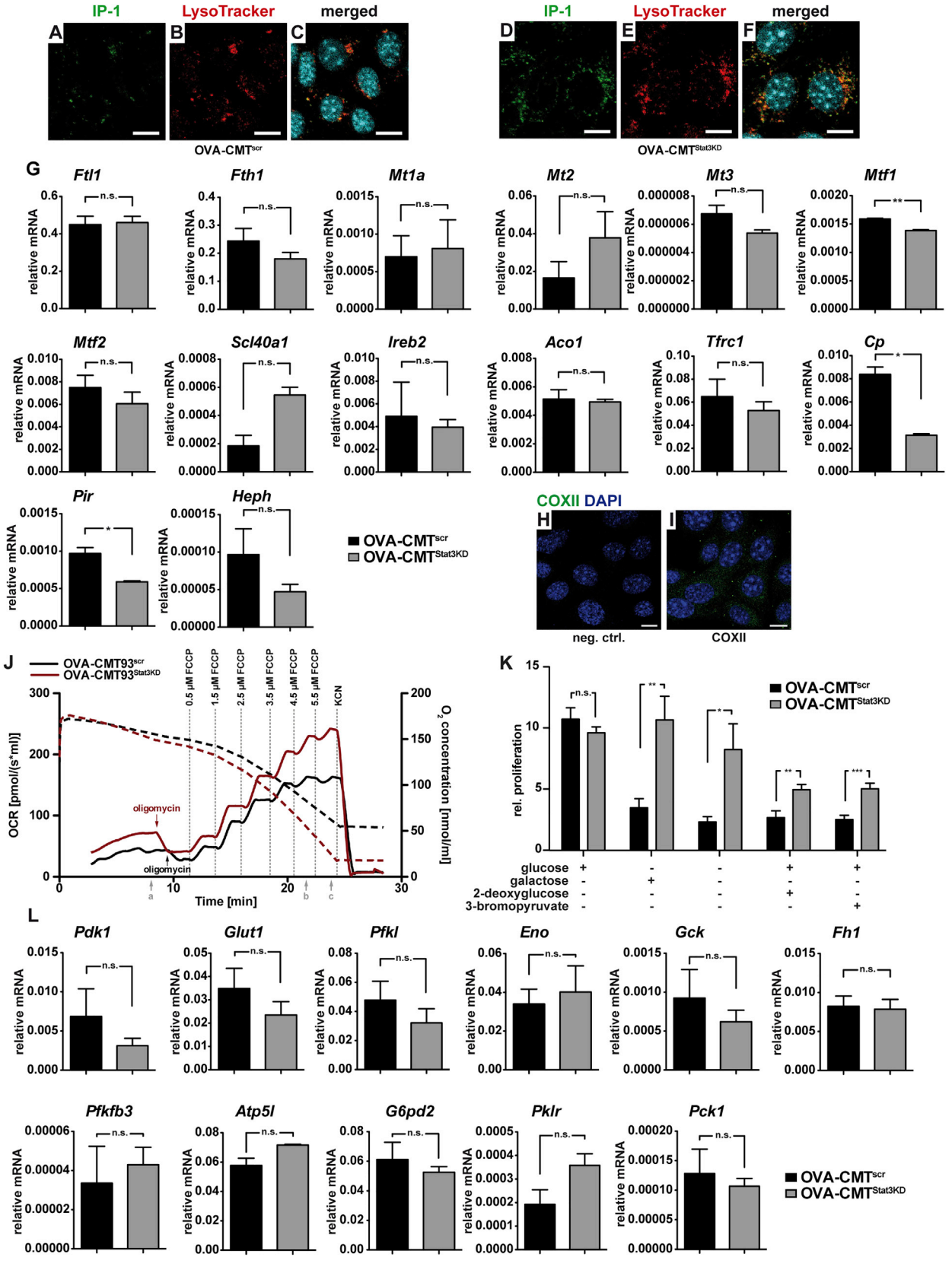

(legend on next page)

Figure S5. Metabolic Alterations in Stat3-Deficient Tumor Cells, Related to Figure 6

(A–F) Confocal live cell microscopy of OVA-CMT^{scr} (E-G) or OVA-CMT^{Stat3KD} cells stained with IP-1 (green) and the lysosomotropic dye LysoTracker (red) to confirm lysosomal localization of iron. Blue staining in the merged images (C and F) represent Hoechst nuclear staining, yellow color indicates co-localization of IP-1 and LysoTracker signal. Scale bar, 10 μm. Please note the depicted sections in (A)–(C) and (D)–(F) represent the same cells than those depicted in Figures S6J and S6K, respectively.

(G) Relative mRNA level of the indicated iron-related gene in OVA-CMT^{scr} or OVA-CMT^{Stat3KD} cells. Data are mean ± SEM, n = 2 each.

(H and I) OVA-CMT cells were stained with control donkey serum (left) or anti-COXII antibody (right) overnight. For staining, AlexaFluor488 conjugated donkey anti-rabbit IgG secondary antibody was used. Scale bar, 10 μm.

(J) Respiratory analysis of the same number of intact cells in FCS-supplemented DMEM. Graph depicting O_2-concentration in dashed lines (right hand scale) and oxygen consumption rate (OCR) in solid lines (left hand scale) during a representative experiment.

(K) Relative proliferation of OVA-CMT^{scr} or OVA-CMT^{Stat3KD} cells in presence or absence of the indicated carbohydrates or inhibitors of glycolysis for 3 days. Data are mean ± SEM, n = 6 of 2 independent experiments, *$p < 0.05$, **$p < 0.01$, ***$p < 0.001$ by Student's t test).

(L) Relative mRNA level of the indicated metabolism related gene in OVA-CMT^{scr} or OVA-CMT^{Stat3KD} cells (Data are mean ± SEM, n = 2 each).

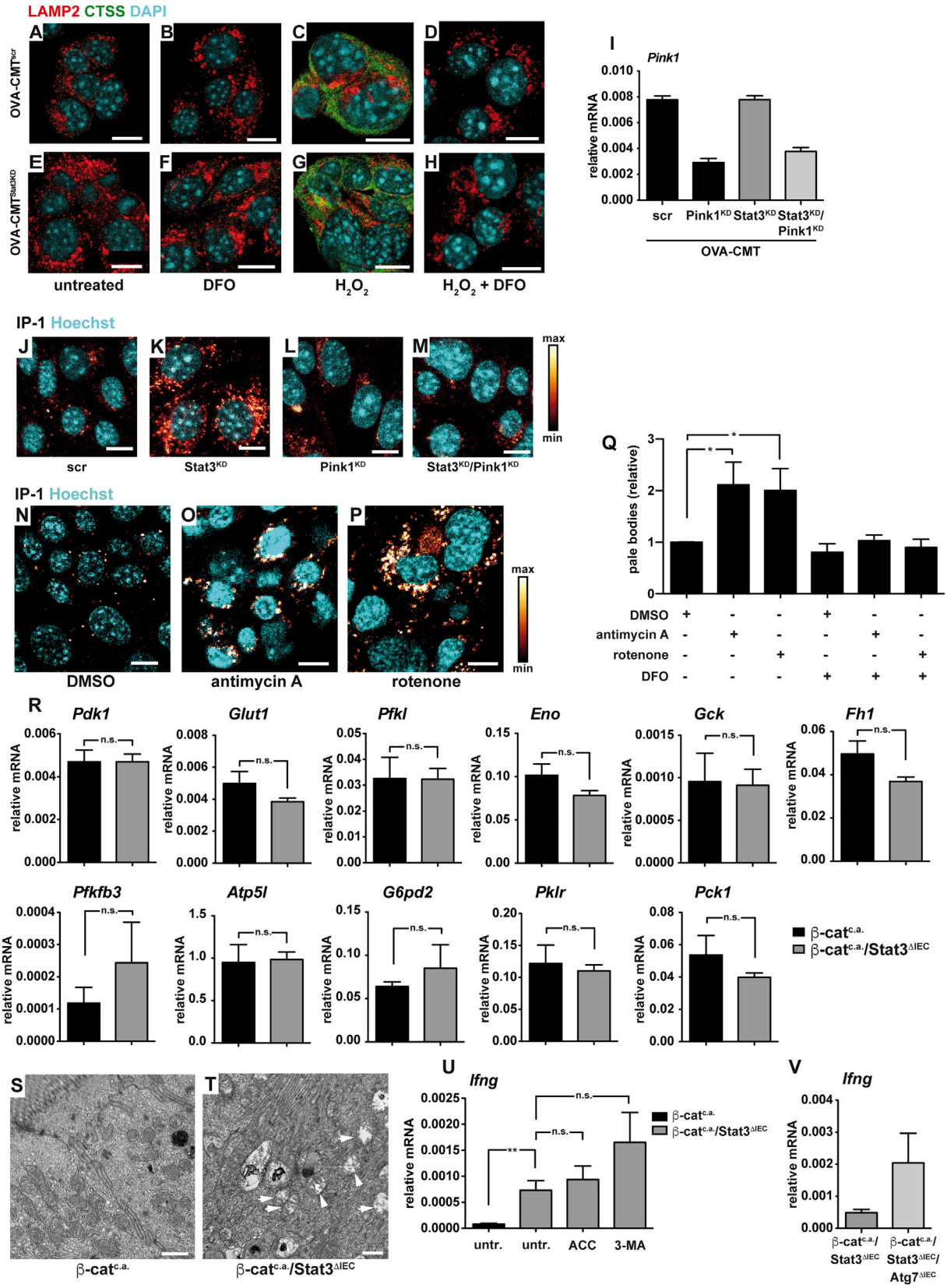

(legend on next page)

Figure S6. Enhanced Mitophagy Triggers LMP suscepTibility in an Iron-Dependent Manner, Related to Figure 7

(A–H) Confocal analysis of immunostainings of OVA-CMT^{scr} (A–D) and OVA-CMT^{Stat3KD} (E–H) cells against cathepsin S (green) and the lysosomal marker LAMP2 (red) after pre-treatment with DFO (1 mM) overnight and H_2O_2 (1 mM) for 2 hr and additional incubation in conventional medium for another 6 hr as indicated. Scale bar, 10 μm.

(I) OVA-CMT cells have been transfected with the indicated siRNA and analyzed 2 days later for the expression of *Pink1*; n = 3 each, bars represent mean ± SEM.

(J–M) Iron content of OVA-CMT cells was measured by confocal live cell microscopy and the fluorescent Fe^{2+}-specific probe IP-1 3 days after transfection with siRNA as indicated. The intensity of IP-1 is shown by a red-yellow LUT depicted on the right hand side. Scale bar, 10 μm.

(N–P) Iron content of OVA-CMT cells was measured by confocal live cell microscopy and the fluorescent Fe^{2+}-specific probe IP-1 after overnight stimulation with antimycin A (100 μM) or rotenone (25 μM). The intensity of IP-1 is shown by a red-yellow LUT depicted on the right hand side. Scale bar, 10 μm.

(Q) Relative fraction of OVA-CMT cells with low red fluorescence upon acridine orange staining (*pale bodies*) as analyzed by flow cytometry. Where indicated cells were incubated overnight with the mitophagy-inducers rotenone (25 μM) or antimycin A (100 μM) or DMSO before incubation with DFO (1 mM) and treated with H_2O_2 (1 mM) for 2 hr and analyzed after 6 additional hours cultured in conventional medium. Data are mean ± SEM, n = 6 of two independent experiments, $^*p < 0.05$ by Student's t test).

(R) Relative mRNA level of the indicated metabolism related gene in IEC of β-*cat*$^{c.a.}$ and β-*cat*$^{c.a.}$/*Stat3*$^{\Delta IEC}$ mice 3 days after the start of tamoxifen administration. Data are mean ± SEM, n = 3 each.

(S and T) Representative electron micrograph of epithelial cells of the small intestine of β-*cat*$^{c.a.}$ (S) and β-*cat*$^{c.a.}$/*Stat3*$^{\Delta IEC}$ (T) mice; arrows = mitochondria undergoing cristolysis, scale bar, 1 μm.

(U) Relative mRNA expression of *Ifng* in small intestinal mucosa of untreated, ACC- or 3-MA treated β-*cat*$^{c.a.}$ and β-*cat*$^{c.a.}$/*Stat3*$^{\Delta IEC}$ mice 15 days after the start of tamoxifen administration. Data are mean ± SEM, n ≥ 3 each.

(V) Relative mRNA expression of *Ifng* in small intestinal mucosa of β-*cat*$^{c.a.}$/*Stat3*$^{\Delta IEC}$ and β-*cat*$^{c.a.}$/*Stat3*$^{\Delta IEC}$/*Atg7*$^{\Delta IEC}$ mice 15 days after the start of tamoxifen administration. Data are mean ± SEM, n = 3 each.